Materials and Structures (2010) 43:1–11
DOI 10.1617/s11527-010-9587-7

ORIGINAL ARTICLE

Effects of sand aggregate on ultrasonic attenuation in cement-based materials

Martin Treiber · Jin-Yeon Kim · Jianmin Qu · Laurence J. Jacobs

Received: 5 April 2009 / Accepted: 15 January 2010 / Published online: 28 January 2010

Abstract Ultrasonic wave attenuation measurements have been successfully used to characterize the microstructure and mechanical properties of inhomogeneous materials; these ultrasonic techniques have the potential to provide for the in-situ characterization of microstructure changes in cement-based materials due to damage. Recent research has applied acoustic scattering models to quantitatively predict ultrasonic attenuation for evaluating the air void content in hardened cement paste. The objective of the current research is to investigate the influence of sand aggregate on the ultrasonic attenuation as a first step towards a full simulation of more realistic microstructures in real concrete. Hardened cement paste samples containing sand aggregate of varying volume fractions are considered. The research employs an independent scattering model and a self-consistent effective medium theory to predict the scattering-induced attenuation of longitudinal ultrasonic waves by the sand inclusions distributed in the cement paste matrix. The predicted attenuation coefficients are compared with measured ones. It is observed that at low volume fractions, both models provide a good estimate of the total attenuation in the specimens. These results indicate that it is possible to use a physics-based model to quantify the effect of sand aggregate on ultrasonic attenuation.

Keywords Ultrasonic testing · Cement-based materials · Ultrasonic attenuation · Acoustic scattering model · Damage in concrete

M. Treiber · J.-Y. Kim (✉) · L. J. Jacobs
School of Civil and Environmental Engineering, Georgia Institute of Technology, Atlanta, GA 30332, USA
e-mail: jykim@gatech.edu

J. Qu · L. J. Jacobs
GWW School of Mechanical Engineering, Georgia Institute of Technology, Atlanta, GA 30332, USA

1 Introduction

Knowledge of the microstructure of cement-based materials can provide valuable information about the macroscopic behavior of these materials. Ultrasonic wave attenuation as a fundamental acoustic parameter of a material can be used to characterize a material's microstructure and therefore help predict the material's performance on the macro scale. Various techniques have been applied in order to assess the structural performance of cement based materials in a nondestructive way. Interesting approaches have been taken, especially for the porosity of concrete as a parameter that is difficult to control in the production process but important for the material's performance [1]. In recent studies, ultrasonic wave attenuation measurements in combination with an acoustic scattering model and an inversion procedure have been successfully used to estimate the content of both entrained and entrapped air voids in hardened cement paste samples [2, 3].

The phenomenon of ultrasonic wave attenuation in hardened and fresh cement-based materials has already been addressed in previous research [4–6]. Materials investigated in these studies are concrete samples that contain coarse aggregates as well as fine aggregates. However, the frequency ranges in these studies were typically below 1 MHz [4], leading to a shortest wavelength about 6 mm, which is about six times larger than the size of sand inclusions ($\sim$1 mm). Since the wave scattering in this long wavelength regime is very small (Rayleigh scattering), the low frequency ultrasound does not have enough sensitivity to characterize the influence of the small inclusions. The current research uses high frequency ultrasound such that wavelengths are comparable to the length scale of the sand particles. On the other hand, cement grains are generally smaller than 50 μm [6]; i.e. the grains are much smaller (approximately one twentieth) than the wavelengths considered in this paper. Thus, in this long wavelength regime, this microscopically inhomogeneous cement paste matrix can be replaced with a homogeneous, viscoelastic material [2, 7]. Jacobs and Owino [8] investigated the effects of aggregate size on the attenuation of laser-generated Rayleigh waves and concluded that aggregate size is not the dominant factor in the ultrasonic attenuation.

Measurements of the wave speed have been successfully applied to characterize the amount of water in concrete, and the evolution of cracks [9]. Research work by Hernández et al. [10, 11] on the modeling of ultrasonic wave propagation in mortars considered the mortar as a three phase material (cement paste, pores and aggregate). However, their micromechanical model focuses on the wave dispersion (thus the static moduli) and considers the cement paste as an elastic material, rather than a viscoelastic one. The model developed by Hernández et al. [10, 11] cannot be used to predict the ultrasonic attenuation. Earlier work [8], Saint-Pierre et al. [12] and Ju et al. [13] have shown that in cement-based materials, ultrasonic attenuation allows for a better characterization of the microstructure than the wave speed measurement.

The current research presents longitudinal wave attenuations for a specimen of pure hardened cement paste (no sand aggregate) in the frequency range 0.5–6 MHz and for specimens with dispersed sand aggregate in the range of 0.8–2 MHz. It is expected that the attenuation in the high frequency range will ultimately provide more information such as size distribution, volume fraction, and interfacial bond strength, and thus should allow for a better characterization of a cement-based material's microstructure at smaller length scales.

The objective of this research is to investigate the influence on the ultrasonic attenuation of relatively fine sand aggregates as they are present in real concrete components, and also to determine how the wave attenuation can be represented by different acoustic scattering models. The research considers mortar specimens with relatively low volume fractions of sand aggregates (9–18.5%). First, the total ultrasonic attenuation of these materials is simulated using two different theoretical models. The ultrasonic attenuation is then measured in four different specimens and the measured attenuation is compared to those predicted with the models. The research analyzes the capability of both models in predicting the scattering behavior of the sand inclusions and in quantifying their effects on the ultrasonic attenuation. Both models are then compared to each other in order to analyze the different resulting predictions. These results are one step in the development of a general technique to characterize the microstructure and damage in cement based materials using the measured attenuation coefficients; they are one step toward a full understanding of how aggregate affect ultrasonic signatures in cement-based materials. The relatively low volume fraction of sand is not the critical aspect, instead what is important is to measure and model attenuation in a real cement-based material, which includes both the paste and aggregate components. A simplified, physical representation like the one proposed in this research will help develop physics-based predictive models for ultrasonic wave propagation in cement-based materials.

The paper is organized as follows: In Sect. 2, the two models, their underlying physical ideas and how these are used to predict the total attenuation are described and then calculated attenuation coefficients are presented. In Sect. 3, the measurement setup and specimens are briefly introduced and the measured attenuation coefficients are shown. Finally, the predictions and measurement results are compared and discussed, and conclusions are drawn.

2 Modeling of coherent wave attenuation

Cement-based materials are inhomogeneous in multiple scales, widely ranging from some nano-meters to a few centimeters. In general, it is not feasible to describe the ultrasonic interaction with the inhomogeneities at all length scales. For example, ultrasonic scattering by nanoscale calcium-silicate-hydrate will require a very complex molecular-level simulation which is currently not available. For this reason, in order to apply a macroscopic ultrasonic scattering model, ultrasonic interactions under a certain length scale needs to be considered phenomenologically and the net effects are accounted for through effective parameters obtained from an experiment. An earlier study [2, 3] considers the cement paste as a homogeneous viscoelastic material, and uses the measured attenuation coefficient as an effective parameter that represents all ultrasonic phenomena in the cement paste matrix in the microscopic scale.

Now, the ultrasonic wave attenuation in a viscoelastic matrix containing randomly distributed particles is caused by two different effects: absorption in the viscoelastic matrix and scattering by the particles. Both of these effects are present in the material under the current investigation. The second effect arises from the scattering of the ultrasonic waves by the sand inclusions. When the wave hits a sand inclusion that is embedded in the cement paste matrix, the wave energy is scattered in many directions that are different from the original direction of propagation. While there is no net energy loss in the scattering process, the wave energy in the direction of propagation looks to be apparently reduced, as much as the energy is scattered in all directions. The attenuation of coherent waves due to scattering by many particles is called the coherent attenuation or the apparent attenuation.

A full mathematical description of the multiple scattering processes is extremely difficult, and numerous approximation models have been proposed. Among others, this research employs two existing, relatively simple scattering models for predicting the attenuation in the cement paste material containing randomly distributed sand inclusions. The first is the independent scattering model [14, 15] while the second follows the self-consistent model proposed by Sabina and Willis [16]. In this study, the sand inclusions are assumed to be spherical in shape and that all inclusions have the same size with a radius a. The sand volume fraction is given as η.

2.1 Independent scattering model

To calculate the amount of energy scattered by randomly distributed inclusions in a homogeneous material, the independent scattering approach has shown to provide useful results for the application of modeling cavities in cement-based materials [2, 3]. Ying and Truell [14] analyzed the scattering of elastic waves by a single sphere and noted that when the volume fraction of scatterers is low, the total scattered field from these multiple inclusions can be predicted by summing up the individual scattered fields by each inclusion. Therefore, the total wave attenuation due to the scattering can then be calculated as a simple summation of the scattering effects of every single scatterer. In this approach, no higher order multiple scattering effects among the inclusions are taken into account. This condition limits the applicability of the model to a low volume fraction, typically below 20%, since at higher volume fractions, scatterer interactions become more and more important and thus need to be accounted for. Brauner and Beltzer [17] used this theory to develop a differential effective medium theory. Biwa [15] improved on this model by removing the volume occupied by the inclusions, so that the material absorption is calculated in a more accurate way. This theory was used to characterize the volume fraction of multi-scale porosity (entrained and entrapped air voids in multiple sizes) in hardened cement paste by Punurai et al. [2, 3, 18].

The total power loss due to scattering by all inclusions is considered with the scattering cross section γ^{sca} of a single inclusion. Following [2, 14, 15], the total attenuation coefficient α for the particulate material is approximated

$$\alpha = (1-\eta)\alpha_{\mathrm{a}} + \frac{1}{2} n_{\mathrm{s}} \gamma^{\mathrm{sca}}, \tag{1}$$

where α_{a} denotes the viscoelastic absorption in the matrix and n_{s} is the number of scatterers per unit volume and is related to the volume fraction η by $\eta = \frac{4}{3}\pi a^3 n_{\mathrm{s}}$ for a spherical inclusion of radius a. The scattering cross section γ^{sca} for the plane longitudinal wave incidence is given by

$$\gamma^{\mathrm{sca}} = 4\pi \sum_{m=0}^{\infty} \frac{1}{2m+1} \left[|A_{\mathrm{m}}|^2 + m(m+1)\frac{c_{\mathrm{l}}}{c_{\mathrm{s}}}|B_{\mathrm{m}}|^2 \right], \tag{2}$$

where c_{l} is the longitudinal wave speed, c_{s} the shear wave speed, m is the mode number, and A_{m} and B_{m} are the coefficients of the series expansions for the longitudinal and shear wave potentials as are given in [14]. Note that A_{m} and B_{m} are a function of frequency and so is γ^{sca}.

2.2 Effective medium model

The second model used in this research is a self-consistent effective medium model described by Sabina and Willis [16] which is a dynamic generalization of the static self-consistent theory of Budiansky [19]. The model defines a homogenization process of an inhomogeneous material. The effective medium theory treats an inhomogeneous material with its acoustic behavior as a homogeneous material defined by a set of yet-unknown overall (effective) material parameters. The model does not directly describe the higher order scattering of waves and their interactions, but instead describes the overall acoustic behavior on a macro scale by solving the scattering problem in an effective medium in a self-consistent manner. The model thus is supposedly suitable for higher volume fractions of inclusions. The self-consistency condition states that the mean wave field in the inhomogeneous material coincides with the wave field propagating in the effective medium [20]. Furthermore, the behavior of the inhomogeneous material with N inclusions can be changed for the effective homogeneous material while each additional single inclusion $N+1$ behaves as an isolated scatterer embedded in the effective medium. With that condition, the multiple scattering problem is reduced to the solution of a single scatterer that is embedded in a material with the effective medium properties. In the literature, many evaluations of these ideas can be found, e.g. in [20, 21].

For a plane incident longitudinal wave, the model finds the effective acoustic parameters for the inhomogeneous material: the two effective elastic constants, $\tilde{\kappa}_{\mathrm{EM}}, \tilde{\mu}_{\mathrm{EM}}$ and the effective elastic density $\tilde{\rho}_{\mathrm{EM}}$. These complex valued ($\tilde{}$) properties are functions of the frequency ω of the incident wave field. With the effective complex dynamic moduli, the effective complex wave numbers ($\tilde{k}_{\mathrm{l}}$ and $\tilde{k}_{\mathrm{s}}$ for longitudinal and shear waves) are calculated.

Finally, the longitudinal wave attenuation of the effective medium can be calculated as the imaginary part of the complex wave number of the longitudinal wave travelling in the effective medium as,

$$\alpha_{\mathrm{l}} = \mathrm{Im}\{\tilde{k}_{\mathrm{l}}\}. \tag{3}$$

Note that in this model, the effect of matrix attenuation enters into the complex wave numbers, and the total attenuation is simply the imaginary part of the effective complex wave number.

2.3 Model results

Both, the independent scattering and effective medium models are applied to predict the longitudinal attenuation coefficient in hardened cement paste samples with different sand volume fractions. Their average diameter is $a = 0.4$ mm and is assumed to be constant for both models. The material properties for both cement paste and quartz sand are listed in Tables 1 and 2. Note that the attenuation in quartz sand is very small and neglected in this study.

The material properties of the cement paste matrix are experimentally determined using the measured values of α_{l} and α_{s}, the measured phase velocities c_{l}, c_{s}, and the measured density ρ [22].

Figures 1 and 2 show respectively, results from the independent scattering model and the effective medium theory. The two models predict quite different attenuations at frequencies higher than

Table 1 Material properties of hardened cement paste[a,b]

Property	Symbol (unit)	Value
Longitudinal wavespeed	$c_{\mathrm{L}}\left(\frac{\mathrm{m}}{\mathrm{s}}\right)$	3680[a]
Shear wavespeed	$c_{\mathrm{S}}\left(\frac{\mathrm{m}}{\mathrm{s}}\right)$	1990[b]
Density	$\rho\left(\frac{\mathrm{Kg}}{\mathrm{m}^3}\right)$	1970[1]
Longitudinal attenuation	$\alpha_{\mathrm{L0}}\left(\frac{\mathrm{Np}}{\mathrm{m}}\right)$	−10.19[a]
$\alpha_{\mathrm{L}}(f) = \alpha_{\mathrm{L0}} + \alpha_{\mathrm{La}} f$	$\alpha_{\mathrm{La}}\left(\frac{\mathrm{Np}}{\mathrm{m \cdot MHz}}\right)$	16.18[a]
Shear attenuation	$\alpha_{\mathrm{S0}}\left(\frac{\mathrm{Np}}{\mathrm{m}}\right)$	8.85[b]
$\alpha_{\mathrm{S}}(f) = \alpha_{\mathrm{S0}} + \alpha_{\mathrm{Sa}} f$	$\alpha_{\mathrm{Sa}}\left(\frac{\mathrm{Np}}{\mathrm{m \cdot MHz}}\right)$	90.46[b]

[a] Values measured in the current research

[b] Values taken from [1]

Table 2 Material properties of quartz sand [31]

Property	Symbol (unit)	Value
Longitudinal wavespeed	$c_L\left(\frac{m}{s}\right)$	5570
Shear wavespeed	$c_S\left(\frac{m}{s}\right)$	3540
Density	$\rho\left(\frac{Kg}{m^3}\right)$	2600
Bulk modulus	κ (GPa)	36.96
Shear modulus	μ (GPa)	32.58

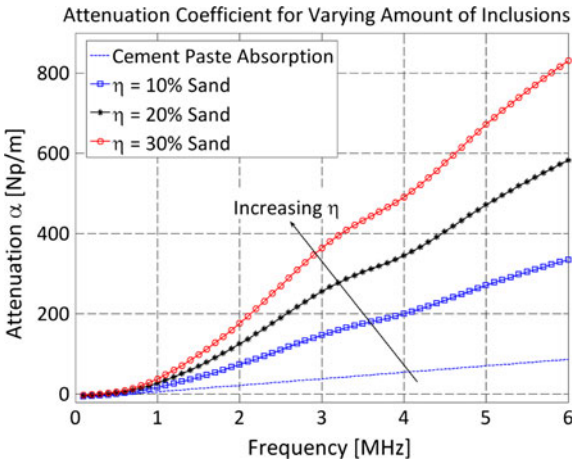

Fig. 1 Attenuation coefficients for the independent scattering model

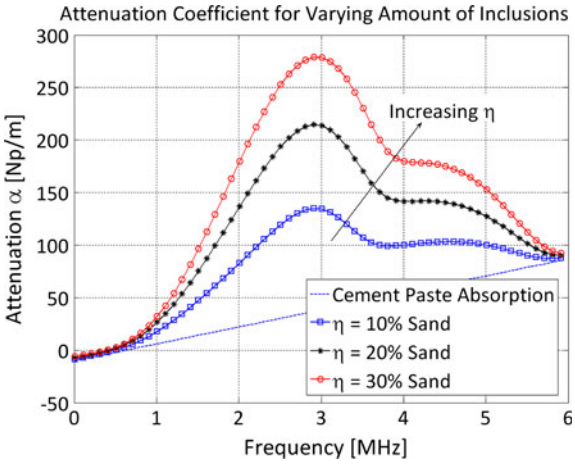

Fig. 2 Attenuation coefficients for effective medium theory model

2 MHz due to the different assumptions in these two theories, while their predictions are coincident below this frequency.

3 Specimens and measurement procedure

The two types of specimens examined in this research are: a single pure cement paste specimen that contains no sand aggregate and three mortar specimens that contain varying amounts of sand aggregate. The pure cement paste specimen is used to characterize the acoustic properties, specifically, the density, the wave speeds and the attenuation coefficients, of the hardened cement paste matrix material in the mortar specimens, while the three mortar specimens are used to examine the influence of the scattering of sand aggregate.

The cement paste specimen is cast from commercial type I Portland cement powder into cylinders of 76.2 mm diameter. The cement powder is mixed with water, at a water-to-cement ratio w/c = 0.4 in weight utilizing a Hobart mixer before a vibration table is used to diminish the amount of entrapped air in the material. The mortar specimens contain different amounts of non-reactive sand, i.e. sand that is chemically treated in order to prevent ASR cracks at the interface with the cement paste matrix material [23]. The sand is sieved between two sieves with nominal grid sizes of 0.76 and 0.841 mm to yield a size distribution between these values. For further investigation, especially regarding the modeling predictions, the radius of the sand inclusions is assumed to be $a = 0.4$ mm and is identical for all sand grains. The grains are assumed to be spherical in shape. Note that the sand aggregate is mixed with the cement powder before contacting it with water in order to ensure a proper mixing condition provided for the aggregate. The volume fractions are 9, 16 and 18.5% for the three aggregate specimens. Since the control of the volume fraction during the casting procedure is cumbersome, the volume fraction is controlled after the molding process using a simple procedure that compares the different densities of the materials and the cast specimens [22].

After 24 h of hydration time in an airtight environment, all specimens are hard enough to be demolded. For another 14 days, they continue to hydrate in a water bath where calcium hydroxide is added to decrease the amount of leaching of calcium hydroxide from the cement itself and to prevent cracking that arises from a chemical alkali-silica reaction (ASR) between the inclusions and the cement paste. From the demolded cylinders, various

specimens are cut with a water cooled diamond saw. The cut specimens are polished with a diamond polishing paper to guarantee that surfaces are flat and parallel to secure a good contact between the measuring transducers and the specimen. It has been shown that the roughness of the coupling surface is important to allow for the transfer of the wave energy into the specimen [24]. To dry the specimens after the polishing process, they are kept in a drying oven at 40°C for 12 h. Note that between each measurement, the specimens are kept in an airtight box at room temperature. The surface of one of the mortar specimens is shown in Fig. 3.

3.1 Measurement procedure

The procedure developed to measure the wave speed and the attenuation coefficient over a broad range of high frequencies (0.8–6 MHz) is a combination of different setups of contact transducer measurements that was specifically developed to measure highly attenuating media and is described in detail in [22, 25]. The general measurement setup is shown in Fig. 4a. Ultrasonic pulses are sent through the specimen using broadband longitudinal transducers with nominal frequencies of 2 and 5 MHz. The frequency spectra of two signals are compared to obtain the attenuation coefficients: the signal of the directly transmitted impulse (Fig. 4b), denoted as S_1, and the signal of the wave that has been reflected on both surfaces of the specimen denoted as S_2 (Fig. 4c). Thus, the attenuation coefficient can be calculated as

$$\alpha(f) = \frac{1}{2z}\left[\ln\left(\left|\frac{S_1(f)}{S_2(f)}\right|\right) - \ln\left(\left|\frac{D(f;z)}{D(f;3z)}\right|\right) + \ln(|R_B R_T|)\right], \quad (4)$$

where z denotes the specimen thickness, $D(f; z)$ is the diffraction correction function proposed by Rogers and Van Buren [26] and R_B and R_T denote the reflection coefficients at the top and bottom interface between the specimen and the transducer whose values vary between zero and unity. The interface coupling conditions may vary quite significantly in each measurement as shown in Fig. 4d, and these are compensated for using in-situ measured reflection coefficients in each measurement. This procedure is described in detail in [25]. The measurement thus corrects for the effects of partial reflection on the interface between the contact transducers and the specimen surface. These effects have not been considered in former research, e.g. [27, 28]. The correction allows for an accurate determination of the absolute ultrasonic attenuation of a material. The specimen thickness z is $\sim$12 mm in this research; for this thickness, the measurement is limited to an upper frequency of 6 MHz for the pure cement paste specimens which are less attenuative. The measurements for the mortars conducted and presented in this paper provide reliable information in a frequency range between 0.8 and 2 MHz. This range is larger for some of the less attenuating media considered in this study.

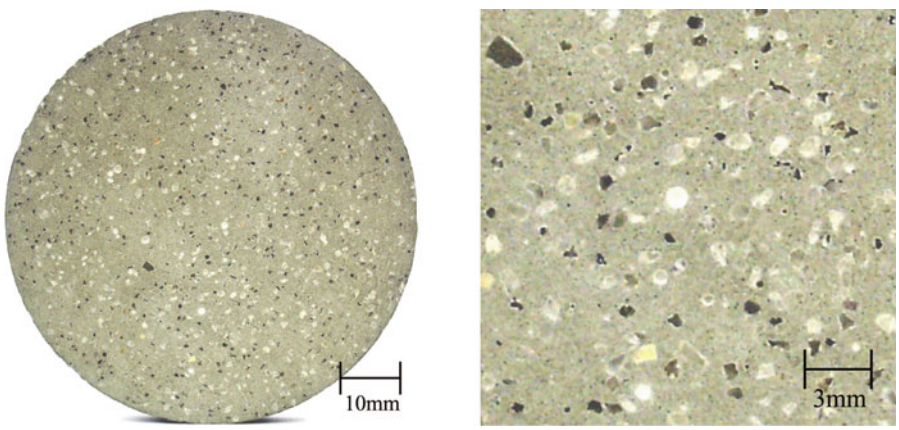

Fig. 3 Sand including specimen with a volume fraction of $\eta = 9\%$

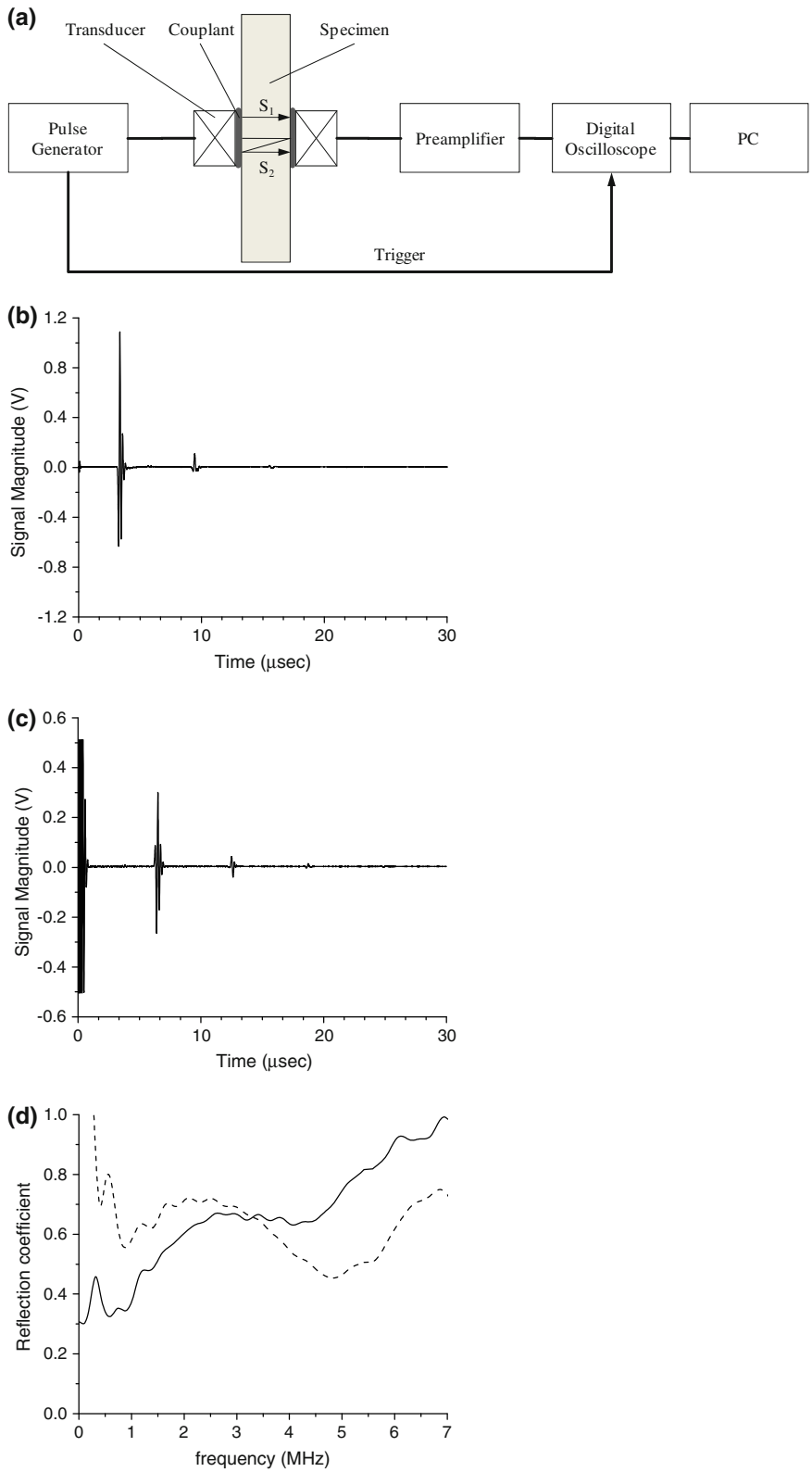

Fig. 4 **a** General measurement setup, **b** direct through transmitted signal, **c** reflected signal, **d** reflection coefficient of the sample-transducer interface, obtained in two different measurements

4 Results

After the attenuation coefficients are measured, the results are compared to the different model predictions and their respective prediction precision is examined.

4.1 Pure cement paste specimen

First, the material properties of the matrix material of the composites—the pure cement paste—are measured. The resulting dispersion curve (wave speed versus frequency) is shown in Fig. 5.

It is observed that cement paste is weakly dispersive in the frequency range considered here. Therefore, the simulations use a representative constant value of $c_l = 3680$ m/s. The attenuation measurement results and the respective error bars of the various measurements are depicted in Fig. 6. Note that the left figure shows error bars from multiple measurements while the right one includes the best linear fit. Clearly, the attenuation in pure cement paste can be well approximated by a linear function. This corresponds to the effect of hysteresis absorption [29, 30] of cement paste that has been observed by Punurai [2, 3]. As discussed earlier, these measured values for the longitudinal phase velocity and attenuation coefficient are input into both the independent scattering and effective medium models to predict the attenuation of the three mortar specimens with varying amounts of sand aggregate. To our knowledge, reliable values of the attenuation coefficient of cement paste up to 6 MHz have not been reported earlier.

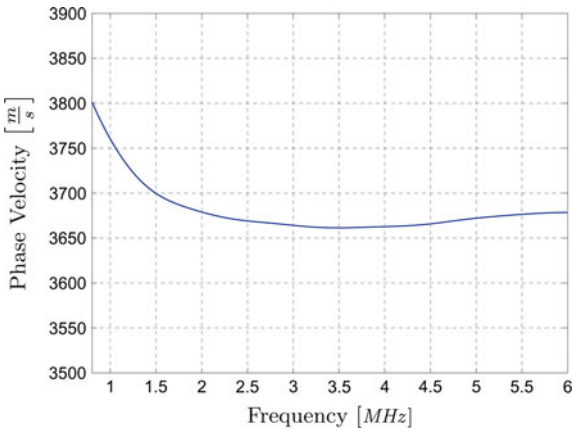

Fig. 5 Phase velocity of longitudinal waves in pure hardened cement paste

4.2 Cement paste specimens with sand aggregate

The measured and simulated wave attenuation coefficients for the three different cement paste specimens with sand aggregate are shown in Figs. 7, 8, 9. The attenuation coefficients are taken as an average of three different measurements carried out at positions over the specimen surface in order to provide more representative values for the randomly distributed sand inclusions.

First, it should be noted that the transducers that are used in this research are band-limited, having a band between 0.8 and 2 MHz. This means that the measured data below this frequency range would be unreliable and likely influenced by extraneous effects. Therefore, the negative valued attenuation is not physical. The undulation in the measured attenuations is due to the coherent noise generated by the multiply scattered waves which smear into the first and second ultrasonic pulse signals. Unlike the incoherent noise that can be significantly reduced by improving instrumentation and the measurement procedure, this noise which is due to the inhomogeneous nature of the material's microstructure cannot be fully removed, while it has been suppressed by properly windowing the pulse signals and taking a spatial average over three locations. The major portion of the coherent noise signal follows closely and overlaps with the tail part of the coherent signal. This major portion can be removed by adjusting the window size. Note that it is inevitable to lose some information of the coherent signal during this operation. The coherent noise is due to the scattering by the randomly distributed scatters along the path of waves between the two transducers. By taking measurements at different locations in the same sample, the coherent noise which is due to the spatial randomness can be suppressed.

It is observed that in general, there is good agreement between the experimentally measured and the predicted attenuation coefficients. Note that the measured attenuation of the pure cement paste specimen is included in all three plots for comparison purposes. As expected, the sand inclusions give rise to higher attenuation over the entire frequency range

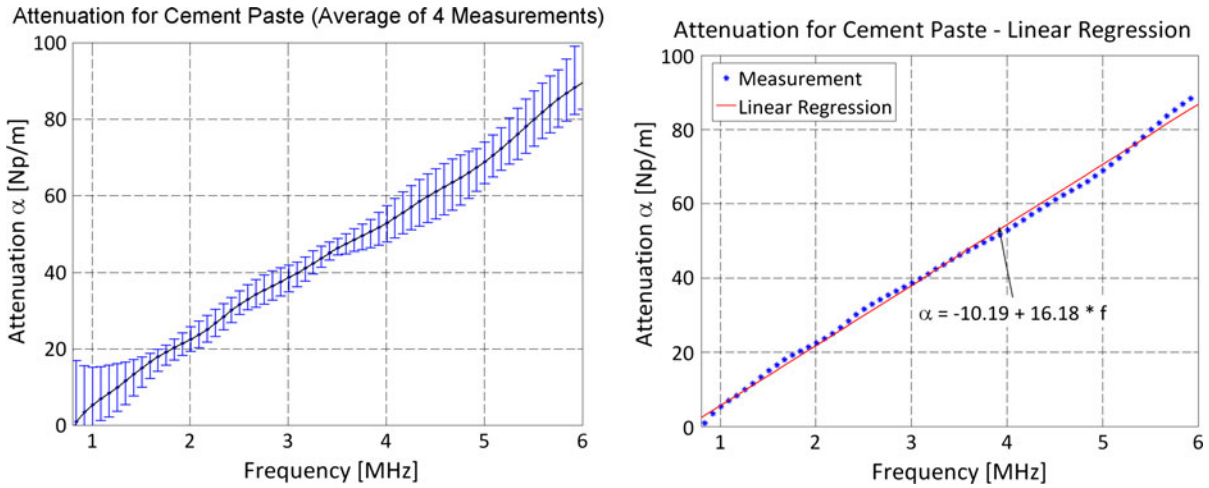

Fig. 6 Attenuation for pure hardened cement paste

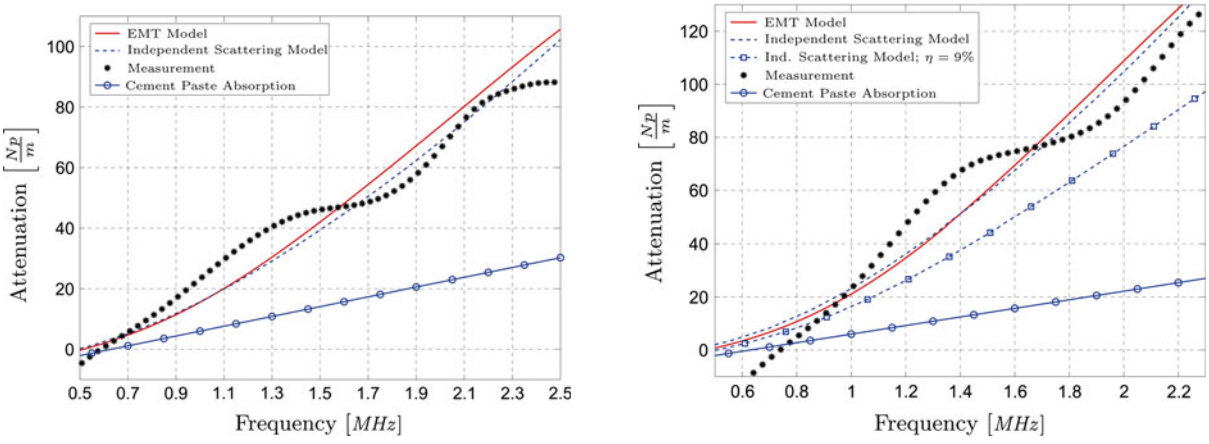

Fig. 7 Attenuation for the cement paste specimen with 9% sand aggregate: measurement and simulation

Fig. 8 Attenuation for the cement paste specimen with 16% sand aggregate: measurement and simulation

due to scattering effects. This effect becomes stronger when the volume fraction of the sand inclusions increases, as can be seen in the generally higher attenuation for the higher volume fractions.

For the frequencies measured in this research, the model predictions are both in a comparable range which lies within the extent of the measurement precision. Thus, the only reliable statement concerning the precision of the prediction of the wave attenuation for the models that can be made is that both models accurately simulate the scattering-induced attenuation in the mortar specimens.

Figure 8 also includes the simulation data of the independent scattering model for $\eta = 9\%$. It is observed that the experimental data are in better agreement with the model predictions for $\eta = 16\%$ than $\eta = 9\%$. Thus, it can be said that the model is capable of distinguishing between two materials with different volume fractions (9 and 16%). Since the modeling results are very comparable to each other, this statement also holds true even if the effective medium model result is not shown. Additionally, Fig. 9 which for comparison purposes also includes the simulation data for the independent scattering model for $\eta = 16\%$ shows that the difference between the two simulations ($\eta = 16\%$ and $\eta = 18.5\%$) lies within the range of the measurement precision. It is clear from this plot that the ultrasonic attenuation is not sensitive enough to distinguish between materials with only small differences in the

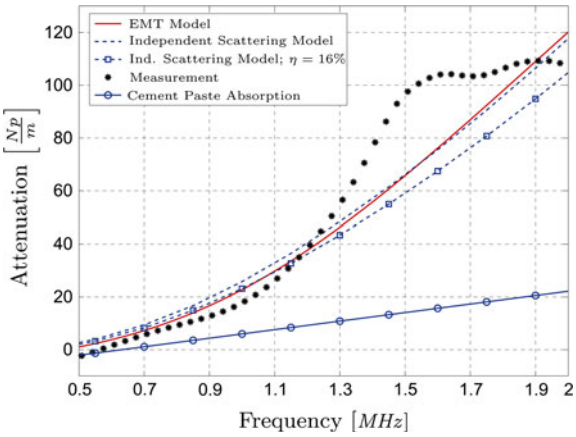

Fig. 9 Attenuation for the cement paste specimen with 18.5% sand aggregate: measurement and simulation

volume fraction of sand aggregate with the measurement setup utilized in this research.

Finally note that the addition of the aggregate will potentially modify the porous structure when compared to the cement paste microstructure. This change in porosity can be due to either the formation of a transition zone in the paste around the aggregate, or the replacement of porous cement paste with less porous aggregate. The influence of the first effect is reduced with the use of use of a fine, natural aggregate, while the second effect is accounted for in both models. The overall combined influence of this modification to the pore structure on attenuation should be a complicated, but higher order effect, which is beyond the scope of this study. However, the attenuation measurements in this study are very consistent, and the overall behavior from paste to increasing volume fraction of fine aggregate behaves as predicted by the physics-based models.

5 Conclusion

This paper presents an experimental and model study on the influence of sand aggregate in cement paste on the attenuation of ultrasonic longitudinal waves. The total ultrasonic attenuation of these particulate materials is simulated using two existing acoustic scattering models. It is observed that in the frequency range used in this study, both models provide comparable results. The attenuation is then measured for mortar specimens with different volume fractions of sand aggregate. There is good agreement between the measured and simulated attenuations in the frequency range under consideration. Computations and measurements show that both models are capable of distinguishing between specimens with largely different volume fractions of sand inclusions (more than 7%). However, small differences in the volume fractions cannot be clearly distinguished with the measurement accuracy and the model sensitivity described in this work. These results indicate that it is possible to use a physics-based model to quantify the effect of sand aggregate on ultrasonic attenuation.

Acknowledgements This work was partially supported by the Georgia Department of Transportation, GTI Project "In Situ Measurement of Air Content in Rigid Pavements" and by the German Academic Exchange Service (DAAD). Their support is greatly appreciated.

References

1. Neithalth N, Weiss WJ, Olek J (2006) Characterizing enhanced porosity concrete using electrical impedance to predict hydraulic and acoustic performance. Cem Concr Res 36(11):2074–2085
2. Punurai W, Jarzynski J, Qu J, Kurtis KE, Jacobs L (2006) Characterization of entrained air voids with scattered ultrasound. NDT&E Int 39:514–524
3. Punurai W, Jarzynski J, Qu J, Kim J-Y, Jacobs J, Kurtis K (2006) Characterization of multi-scale porosity in cement paste by advanced ultrasonic techniques. Cem Concr Res 37:38–46
4. Philippidis T, Aggelis D (2005) Experimental study of wave dispersion and attenuation in concrete. Ultrasonics 43:584–595
5. Aggelis D, Polyzos D, Philippidis T (2005) Wave dispersion and attenuation in fresh mortar: theoretical predictions vs. experimental results. J Mech Phys Solids 53:857–883
6. Neville A (1995) Properties of concrete. Longman, London
7. Christensen RM (1979) Mechanics of composite materials. Wiley, New York
8. Jacobs LJ, Owino JO (2000) Effects of aggregate size on attenuation of rayleigh waves in cement-based materials. J Eng Mech 126(11):1124–1130
9. Popovics S (2005) Effects of uneven moisture distribution on the strength of and wave velocity in concrete. Ultrasonics 43:429–434
10. Hernández M, Anaya J, Ullate L, Ibañez A (2006) Formulation of a new micromechanic model of three phases for ultrasonic characterization of cement-based materials. Cem Concr Res 36:609–616
11. Hernández M, Anaya J, Ullate L, Cegarra M, Sanchez T (2006) Application of a micromechanical model of three phases to estimating the porosity of mortar by ultrasound. Cem Concr Res 36:617–624

12. Saint-Pierre F, Rivard P, Ballivy G (2007) Measurement of alkali–silica reaction progression by ultrasonic waves attenuation. Cem Concr Res 37:948–956
13. Ju J, Weng L, Liu Y (2006) Ultrasonic frequency-dependent amplitude attenuation characteristics technique for nondestructive evaluation of concrete. ACI Mater J 103(M20):177–185
14. Ying C, Truell R (1956) Scattering of a plane longitudinal wave by a spherical obstacle in an isotropically elastic solid. J Appl Phys 27:1086–1097
15. Biwa S (2001) Independent scattering and wave attenuation in viscoelastic composites. Mech Mater 33:635–647
16. Sabina F, Willis J (1988) A simple self-consistent analysis of wave propagation in particulate composites. Wave Motion 10:127–142
17. Brauner N, Beltzer A (1988) Wave-obstacle interaction in a lossy medium: energy perturbations and negative extinction. Ultrasonics 26:328–334
18. Punurai W (2006) Cement-based materials' characterization using ultrasonic attenuation. PhD Dissertation, Georgia Institute of Technology
19. Budiansky B (1965) On the elastic moduli of some heterogeneous materials. J Mech Phys Solids 13:223–234
20. Kanaun S, Levin V, Sabina FJ (2004) Propagation of elastic waves in composites with random set of spherical inclusions (effective medium approach). Wave Motion 40:69–88
21. Kim J-Y, Ih J-G, Lee B-H (1995) Dispersion of elastic waves in random particulate composites. J Acoust Soc Am 97:1380–1388
22. Treiber M (2008) Characterization of cement-based multiphase materials using ultrasonic wave attenuation. Master Thesis, Georgia Institute of Technology
23. Kurtis K, Collins C, Monteiro P (2002) The surface chemistry of the alkali-silica reaction: a critical evaluation and x-ray microscopy. Concr Sci Eng 4(13):2–11
24. Tharmaratnam K, Tan B (1990) Attenuation of ultrasonic pulse in cement mortar. Cem Concr Res 20(3):335–345
25. Treiber M, Kim J-Y, Jacobs L, Qu J (2009) Correction for partial reflection in ultrasonic attenuation measurements using contact transducers. J Acoust Soc Am 125(5):2946–2953
26. Rogers PH, Van Buren AL (1974) Exact expression of Lommel diffraction correction integral. J Acoust Soc Am 55(4):724–728
27. Goueygou M, Piwakowski B, Ould Naffa S, Buyle-Bodin F (2002) Assessment of broadband ultrasonic attenuation measurements in inhomogeneous media. Ultrasonics 40:77–82
28. Sears F, Bonner B (1981) Ultrasonic attenuation measurement by spectral ratios utilizing signal processing techniques. IEEE Trans Geosci Remote Sens GE-19:95–99
29. Rose J (1999) Ultrasonic waves in solid media. Cambridge University Press, Cambridge
30. Hartmann B, Jarzynski J (1972) Ultrasonic hysteresis absorption in polymers. J Appl Phys 43:4304–4312
31. Nadeau J (2002) Water cement ratio gradients in mortars and corresponding effective elastic properties. Cem Concr Res 32:481–490